Plant Stress 11 (2024) 100368

Contents lists available at ScienceDirect

Plant Stress

journal homepage: www.sciencedirect.com/journal/plant-stress

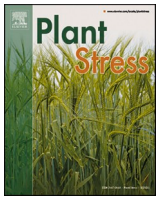

Comparative transcriptome analysis of respiration-related genes in nodules of phosphate-deficient soybean (*Glycine max* cv. Williams 82)

Saad Sulieman [a,*], Chien Van Ha [b], Dung Tien Le [c,1], Mostafa Abdelrahman [b], Cuong Duy Tran [d], Yasuko Watanabe [e], Maho Tanaka [f,g], Zaid Ulhassan [h], Mohamed S. Sheteiwy [i,j], Sunil S. Gangurde [k], Keiichi Mochida [e,l,m,n], Motoaki Seki [f,g,m], Lam-Son Phan Tran [b,*]

[a] *Department of Agronomy, Faculty of Agriculture, University of Khartoum, Shambat, Khartoum North 13314, Sudan*
[b] *Institute of Genomics for Crop Abiotic Stress Tolerance, Department of Plant and Soil Science, Texas Tech University, Lubbock, TX 79409, USA*
[c] *VKTECH Research Center, NTT Hi-Tech Institute, Nguyen Tat Thanh University, 298A-300A Nguyen Tat Thanh Street, District 4, Ho Chi Minh City, 70000, Viet Nam*
[d] *Genetic Engineering Department, Agricultural Genetics Institute, Vietnamese Academy of Agricultural Science, Pham Van Dong Street, Hanoi 100000, Viet Nam*
[e] *Bioproductivity Informatics Research Team, RIKEN Center for Sustainable Resource Science, Yokohama 230-0045, Japan*
[f] *Plant Genomic Network Research Team, RIKEN Center for Sustainable Resource Science, 1-7-22 Suehiro-cho, Tsurumi-ku, Yokohama, Kanagawa 230-0045, Japan*
[g] *Plant Epigenome Regulation Laboratory, RIKEN Cluster for Pioneering Research, 2-1 Hirosawa, Wako, Saitama 351-0198, Japan*
[h] *Institute of Crop Science, Ministry of Agriculture and Rural Affairs Key Laboratory of Spectroscopy Sensing, Zhejiang University, Hangzhou 310058, China*
[i] *Department of Integrative Agriculture, College of Agriculture and Veterinary Medicine, United Arab Emirates University, P.O. Box 15551, Al Ain, Abu Dhabi, UAE*
[j] *Department of Agronomy, Faculty of Agriculture, Mansoura University, Mansoura 35516, Egypt*
[k] *International Crops Research Institute for the Semi-Arid Tropics, Hyderabad 502324, India*
[l] *School of Information and Data Sciences, Nagasaki University, 1-14 Bunkyo-machi, Nagasaki 852-8521, Japan*
[m] *Kihara Institute for Biological Research, Yokohama City University, 641-12 Maioka-cho, Totsuka-ku, Yokohama, Kanagawa 244-0813, Japan*
[n] *RIKEN Baton Zone Program, 1-7-22 Suehiro-cho, Tsurumi-ku, Yokohama 230-0045, Japan*

ARTICLE INFO

Keywords:
Acclimatization
Bradyrhizobium diazoefficiens
Carbon metabolism
Gene expression
Glycine max
Phosphorus

ABSTRACT

A transcriptome analysis was used to compare the nodule transcriptomes of the model soybean 'Williams 82' inoculated with two *Bradyrhizobium diazoefficiens* strains (USDA110 vs. CB1809) under phosphate (Pi) deficiency. The entire dataset revealed a core set of low-Pi-responsive genes and recognized enormous differential transcriptional changes between the Pi-deprived USDA110-nodules and CB1809-nodules. The lower symbiotic efficiency of the Pi-starved USDA110 nodules was ascribed to the downregulation of an *F1-ATPase* gene engaged in oxidative phosphorylation, more likely contributing to diminished ATP production. To cope with energy shortage caused by Pi stress, the Pi-deprived USDA110-nodules preferentially upregulated the expression of a large number of genes encoding enzymes implicated in specialized energy-demanding pathways, such as the

Abbreviations: 2HGD, 2-hydroxyglutarate dehydrogenase; AAE/ACN, acetate-CoA ligase; acetyl-CoA, acetyl-coenzyme A; ADH, alcohol dehydrogenase; ALDH, aldehyde dehydrogenase; AMY, α-amylase; bHLH, basic helix loop-helix; bZIP, basic-leucine zipper; AOX, alternative oxidase; BMY/BAM, β-amylase; C, carbon; CA, carbonic anhydrase; COX, cytochrome c oxidase; C2C2(ZN) DOF, DNA binding with one finger-like; DAS, day after sowing; DEGs, differentially expressed genes; DHAP, dihydroxyacetone phosphate; DME, NAD^+-malic enzyme; mETC, mitochondrial electron transport chain; ETF, electron transfer flavoprotein; ETFQO, flavoprotein:ubiqionone oxidoreductase; FDR, false discovery rate; F-1,6-P_2, fructose-1,6-bisphosphate; F6P, fructose-6-phosphate; GABA, γ-aminobutyric acid; GAD, glutamate decarboxylase; GAPC, glyceraldehyde-3-phosphate dehydrogenase; glycerate-1,3-P_2, glycerate-1,3-biphosphate; glycerate-2-P, glycerate 2 phosphate; glyceraldehyde-3-P, glycerate-3-phosphate; G1P, glucose-1-phosphate; G6P, glucose-6-phosphate; HXK, hexokinase; IVD, isovaleryl-CoA dehydrogenase; KEGG, Kyoto Encyclopedia of Genes and Genomes; LP, low-Pi; MAPK, mitogen-activated protein kinase; MDH, malate dehydrogenase; ME, malic enzyme; MLS, malate synthase; MYB/HD-like, myeloblastosis/homeodomain-like; N, nitrogen; NAC, no apical meristem/*Arabidopsis* transcription activation factor 1 and 2/cup-shaped cotyledon; NDI, NAD(P)H type II dehydrogenase; PDC, pyruvate decarboxylase; PDK, pyruvate dehydrogenase kinase; PEP, phosphoenolpyruvate; PEPC, phosphoenolpyruvate carboxylase; PFK, phosphofructokinase; PHB, poly-β-hydroxybutyrate; PK, pyruvate kinase; PPCK, phosphoenolpyruvate carboxykinase; PPI, protein-protein interaction; PPi, pyrophosphate; Pi, inorganic phosphate; qRT-PCR, quantitative real-time-polymerase chain reaction; SBE, starch-branching enzyme; SBP, SQUAMOSA promoter binding protein; SP, sufficient-Pi; SS, starch synthase; SUS, sucrose synthase; TCP, teosinte branched 1, cycloidea, PCF; TF, transcriptional factor; Tg, teragrams; TME, $NADP^+$-malic enzyme; UCP, uncoupling protein; UDP, uridine diphosphate; UGPase, UDP–glucose pyrophosphorylase; UQ, ubiquinone; W82, Williams 82; YEM, yeast extract mannitol.

* Corresponding authors.
E-mail addresses: saadsulieman@hotmail.com (S. Sulieman), son.tran@ttu.edu (L.-S.P. Tran).
[1] Current address: Bayer Viet Nam Limited, 106 Nguyen Van Troi, Phu Nhuan District, Ho Chi Minh City, Viet Nam.

https://doi.org/10.1016/j.stress.2024.100368
Received 18 October 2023; Received in revised form 21 December 2023; Accepted 18 January 2024
Available online 19 January 2024

mitochondrial respiratory chain (i.e., cytochrome c oxidase), alcoholic fermentation (i.e., pyruvate decarboxylase and alcohol dehydrogenase) and glycolysis (e.g., hexokinase, phosphofructokinase, glyceraldehyde-3-phosphate dehydrogenase and pyruvate kinase). These respiratory adjustments were likely associated with higher metabolic cost and redox imbalance, thereby, negatively affecting nodule symbiosis under Pi deprivation. In contrast, the Pi-starved CB1809-nodules reduced the metabolic cost by regulating a lower number of genes and increasing the expression of genes encoding proteins implicated in non-phosphorylating bypasses (e.g., flavoprotein alpha and flavoprotein:ubiqionone oxidoreductase), which could promote the carbohydrate utilization efficiency and energy metabolism. Notably, the upregulation of a transcript encoding a malate dehydrogenase could boost the CB1809-nodules under Pi stress. The dynamic shifts in energy metabolism in the Pi-deprived USDA110-nodules and CB1809-nodules could be transformative to upgrade the mechanistic/conceptual understandings of soybean adaptation to Pi deficiency at the transcriptional level.

1. Introduction

Soybean is an essential commercial crop widely cultivated in different parts of the world (Toomer et al., 2023). The principal cultivated areas of this crop are primarily focused in North America, South America and Asia, which have been expanded into new regions (e.g., Europe) that were not formerly used for large-scale production (Liu et al., 2019; Nendel et al., 2023). The substantial expansion in soybean production is mainly ascribed to the escalating interest in dietary lipids and proteins, which can reach up to 20% and 40% of seed weight, respectively (Wiederstein et al., 2023; Zhong et al., 2023). As a result, soybean has been considered the foremost provider of both products in the global economy. The protein constituents of soybeans are rich and relatively cheap compared with other dietary sources. Thus, soybean remains an enormous economic source of human nutrition and livestock feedstuff, especially in Asia (Liu et al., 2019; Mo et al., 2022). Importantly, soybean contains diverse bioactive molecules, which can promote human health and reduce the incidence of many problems, e.g., high cholesterol levels, and cerebrovascular and cardiovascular diseases (Foyer et al., 2019). Due to their healthy and high nutritional values, numerous high-quality food products (e.g., soy cheese, soy milk, tempeh and tofu) are manufactured today from soybean proteins (Wiederstein et al., 2023). The extracted lipids are increasingly used in various human (e.g., cooking oils, margarine, fried and baked food products) and industrial (e.g., hydraulic fluids, lubricants, plastics, fatty acids and biodiesel) commodities. In addition, many countries are highly interested in cultivating soybeans as a cheap and sustainable source for biodiesel production (Subramanian and Smith, 2013).

In addition to the numerous potential health and economic advantages, soybean is well-known to form highly-specialized symbiotic associations with a group of gram-negative diazotrophic α-proteobacteria that belong to *Bradyrhizobium* (*B. diazoefficiens, B. lianingense* and *B. elkani*), *Mesorhizobium* (*M. tianshanense*) or *Sinorhizobium* (*S. xinjiangense* and *S. fredii*) genus (Ohyama et al., 2011). Among these genera, the strains belonging to *B. diazoefficiens* (formerly known as *B. japonicum*) are the most studied symbiotic bacteria (Sulieman et al., 2022). On average, the efficiency of symbiosis with N_2-fixing bacteria can fulfill 50–60% of the overall potential nitrogen (N) demand of the host plant (Subramanian and Smith, 2013). However, it can reach up to 100% depending on the cultivar, microsymbiont partner (rhizobial strain) and the surrounding growth conditions. It has been estimated that soybeans can fix 16.4 teragrams (Tg) N annually (Zhong et al., 2023). This amount corresponds to approximately 77% of the total fixed N by other legumes. Soybean contributes significantly to the development of sustainable agriculture, thus minimizing the overdependence on expensive synthetic fertilizers, adversely affecting water resources, i.e., eutrophication.

Although soybean has a superior capacity to fix N_2 with soil rhizobia (Chen et al., 2019), unfortunately, the symbiotic relationship between soybean and rhizobia is highly sensitive to a wide range of edaphic and climatic conditions (Zhong et al., 2023). Among the various adverse conditions, inorganic phosphate (Pi) starvation appears to be a major nutritional constraint that profoundly hinders soybean growth and productivity (Yao et al., 2022). The vast majority of soils in different parts of the world has been characterized as Pi-deficient; and thus, cannot support the sustainable crop production systems (Zhang et al., 2019, 2021). The suboptimal-Pi availability in soils is further compounded by the current and future predicted shortage in global rock-Pi reserves used to synthesize Pi-containing fertilizers (Approaching Peak Phosphorus, 2022). This situation can adversely affect soybean growth and productivity, especially when plants evolve nodule symbiosis with soil-borne diazotrophic rhizobia (Liu et al., 2018). Unsurprisingly, N_2-fixing plants require remarkable Pi to fuel nodule growth and function (Chen et al., 2019). Under such circumstances, nodule symbiosis could markedly increase the amount of Pi required to sustain plants' different cellular metabolic processes (Sulieman et al., 2022).

To cope with these adverse conditions, Pi-starved soybean plants have evolved a complex suite of acclimatization strategies, which can assist plants to ameliorate the negative impacts of cellular-Pi deficiency and enable them to survive under severely Pi-impoverished conditions (Liu et al., 2018). Due to the complex nature of cellular metabolism, it has not yet been possible to fully characterize the primary candidates, contributing to low-Pi acclimatization, especially in symbiotic soybean plants (Yao et al., 2022). Soybean represents an important platform that can significantly assist in elucidating the different acclimatization mechanisms used to cope with Pi deficiency. The complete genome sequencing of the model cultivar Williams 82 (W82) (Schmutz et al., 2010) and its symbiotic bacterium *B. diazoefficiens* strain USDA110 (Kaneko et al., 2002) makes soybean an excellent platform for this kind of study. Accordingly, it is very timely to elucidate the genetic and molecular mechanisms of soybean tolerance that underpin nodule organogenesis and functionality under limited Pi availability. These advances can significantly assist in developing superior cultivars with higher and long-lasting symbiotic efficiency under low-Pi conditions.

This study aimed to explore the transcriptome-wide changes induced by Pi deficiency in W82 nodules and to identify the genetic components involved in the apparent low- or high-symbiotic efficiency during Pi starvation. Even nodule respiration is well-known to affect soybean nodulation under Pi deficiency at physiological level, its functional role has not been well elucidated at the transcriptional level during Pi-stress conditions. The identification of metabolic pathways and gene networks affecting nodule respiration is of utmost importance for the following specific reasons: (i) symbiotic nodules represent a large sink of photosynthates (~ 40% of photoassimilates), which are required to sustain the energy transducing pathways and subsequent metabolic activities (Vauclare et al., 2010), (ii) respiration is the primary metabolic process that orchestrates the nodule response to low-Pi stress (Lazali et al., 2017), (iii) respiration is a dynamic process encompassing very flexible strategies, which should be explored in Pi-deprived nodules (Sulieman et al., 2022), (iv) carbohydrates and associated higher respiratory activities are closely connected with other vital metabolic processes (e.g., O_2 consumption, N assimilation and export and cellular redox balance) in nodules (Valentine et al., 2017).

2. Materials and methods

2.1. Growth conditions and experimental design

Soybean (*Glycine max* [L.] Merrill) cv. W82 was germinated on autoclaved vermiculite in plastic pots (6 liters) and cultured inside a greenhouse, as described by Sulieman et al. (2019). Soybean plants were irrigated with full-strength Herridge's solution containing either low-Pi (LP) or sufficient-Pi (SP) in the form of KH_2PO_4 (basal nutrient solution containing 0.1 mM or 2.0 mM of Pi, respectively). Germinating plants were employed with two *B. diazoefficiens* strains (USDA110 vs. CB1809), revealing differential Pi responses at the metabolite level (Sulieman et al., 2019). The USDA110 strain has been proposed as a model microsymbiont to dissect the physiological and molecular mechanisms involved in soybean-rhizobia symbioses (Kaneko et al., 2002). The experimental setup depicted in Supplementary Fig. S1 allows us to compare the transcriptome analysis of CB1809- and USDA110-related nodules at LP and SP conditions. Nodule samples were collected at 35 DAS (day after sowing), flash-frozen in liquid N_2 and kept at −80°C until RNA isolation.

2.2. Total RNA extraction and quality assurance for gene expression analysis

Total RNA was isolated from the resulting frozen nodules using Trizol reagent (Invitrogen, Carlsbad, CA, USA) following the manufacturer's experimental manual. Subsequently, extracted RNA samples were digested with DNAse I (Qiagen, Nordrhein-Westfalen, Germany). The RNA samples were passed through quality control criteria using a Nanodrop spectrophotometer and Agilent 2100 Bioanalyzer (Agilent Technologies) as described elsewhere (Le et al., 2012a). Finally, total RNA was stored frozen (−80°C) until the transcriptome analysis and quantitative real-time polymerase chain reaction (qRT-PCR) were performed using three independent biological replicates for each treatment.

2.3. Transcriptome analysis

cDNA libraries were constructed using the Ambion WT Expression Kit (Life Technology, Carlsbad, CA, USA) as recommended by the manufacturer's procedure. The cDNAs were fragmented and labeled following the experimental manual of the Affymetrix GeneChip WT Terminal Labeling Kit (Affymetrix, Santa Clara, CA, USA). Labelled cDNAs were hybridized (66K), and obtained raw data were analyzed following the procedure described by Le et al. (2012a). All data were deposited to the public NCBI-Gene Expression Omnibus (NCBI-GEO) repository database (www. ncbi.nlm.nih.gov/geo/browse/?view=series) under the accession number GSE244933. The transcriptome data were annotated, analyzed and visualized using MapMan (https://mapman.gabipd.org/mapman) software (Thimm et al., 2004; Usadel et al., 2009).

2.4. Kyoto Encyclopedia of Genes and Genomes (KEGG) pathways, transcriptional factor (TF) enrichment and protein-protein interaction (PPI) networks

A Venn diagram, generated using the default settings of the Bioinformatics and Evolutionary Genomics web-based tool (https://bioinformatics.psb.ugent.be/webtools/Venn/), was employed to discern the number of overlapping and unique differentially expressed genes (DEGs) in the 'USDA110-LP vs. USDA110-SP' and 'CB1809-LP vs. CB1809-SP' comparisons. Subsequently, both the overlapping and specific DEGs from these comparisons were analyzed for KEGG pathway enrichment using ShinyGO v0.77 (https://bioinformatics.sdstate.edu/go/), with *G. max* as the reference species. Protein-protein interaction (PPI) networks were constructed using multiple protein identifiers in STRING (https://string-db.org/). Finally, we identified all genes encoding TFs among the DEGs across different comparisons. This was achieved by a search using DEG IDs as queries in the PlantRegMap function in PlantTFDB (https://planttfdb.gao-lab.org/). Next, the identified TF-encoding genes, which possess significantly overrepresented targets in our query DEG IDs, were filtered out using Fisher's test ($p < 0.05$). The overrepresented TF-encoding genes were further subjected to transcriptional regulatory enrichment analysis using Plant GeneSet Annotation Database (Plant GSAD, https://systemsbiology.cau.edu.cn/PlantGSEAv2/).

2.5. qRT-PCR

For the validation of the transcriptome data, seven genes (*Glyma.13G191600, Glyma.09G225400, Glyma.13G056600, Glyma.03G131700, Glyma.10G201100, Glyma.05G179800* and *Glyma.12G234200*) were randomly selected and analyzed by qRT-PCR following the established procedure (Le et al., 2012b). The gene-specific primer pairs used for qRT-PCR are shown in Supplementary Table S1. The qRT-PCR analysis was performed as previously described using three independent biological replicates per sample in conjugation with the *Fbox* gene as a housekeeping reference gene (Le et al., 2012b).

2.6. Statistical analysis

The Student's *t*-test (*p*-value cutoff at 0.05) was applied for comparison between paired contrasts (LP-treated vs. corresponding SP-treated control) for each transcript. Correction of the *p*-values (*q*-values) was processed by calculating the false discovery rate values [false discovery rate (FDR cutoff at 0.05)] according to the Benjamini and Hochberg adjustment method (Le et al., 2012a). The criteria of *q*-value < 0.05 and ≥ 2-fold difference in expression were used to detect the DEGs. As for the qRT-PCR, statistical analysis was performed using Student's *t*-test at a 95% confidence level.

3. Results and discussion

3.1. Transcriptome analysis reveals differential gene expression patterns in the nodules colonized by the B. diazoefficiens USDA110 and CB1809 strains under LP

Our recently published non-targeted GC-TOF/MS-based metabolite profiling revealed differential metabolite arrangements in the Pi-starved nodules colonized by USDA110 and CB1809 strains (Sulieman et al., 2019). For comparative transcriptome analysis, the 66K soybean GeneChip (Supplementary Table S2) was used following the experimental setup depicted in Supplementary Fig. S1, which allowed us to compare the transcriptomes of CB1809- and USDA110-related nodules in four pairwise contrasts: USDA110-LP/USDA110-SP, CB1809-LP/CB1809-SP, CB1809-SP/USDA110-SP and CB1809-LP/USDA110-LP. Nevertheless, the present report described the gene expression changes in USDA110-LP/USDA110-SP and CB1809-LP/CB1809-SP with more emphasis on the differential effects of USDA110 and CB1809 on gene expression in soybean nodules under LP vs. SP conditions. This approach could help us understand the expression patterns of genes contributing to nodule tolerance during Pi deprivation. By employing the Glyma v2.0 annotation, we could explore the expression levels of 38,172 genes with high confidence. The criteria of *q*-value < 0.05 and ≥ 2-fold difference in expression levels were used to detect the DEGs (Supplementary Table S3). The transcriptome profiling corroborates with the metabolome data (Sulieman et al., 2019) and provides further in-depth knowledge of the existing strategies by which nodules could tolerate Pi deprivation. Based on the comparative analysis, Pi scarcity induced large-scale re-programming of gene expression in nodules (Supplementary Fig. S2), as mirrored by the significant alterations of a total number of 1823 and 645, in USDA110-LP/USDA110-SP and

CB1809-LP/CB1809-SP, respectively (Supplementary Fig. S3). In particular, 667 (37%) vs. 263 (41%) genes were upregulated, while 1156 (63%) vs. 382 (59%) genes were downregulated in USDA110-LP/USDA110-SP vs. CB1809-LP/CB1809-SP, respectively (Supplementary Fig. S3; Supplementary Table S4A-D). The qRT-PCR analysis of several genes, including *Glyma.10G201100* putatively encoding pyruvate kinase (PK) that plays a prominent role in determining the efficiency of nodule symbiosis under Pi stress (Liu et al., 2018), confirmed the precision of the transcriptome analysis as depicted in Supplementary Fig. S4.

MapMan analysis demonstrated that USDA110-LP/USDA110-SP altered transcriptional changes in considerably higher number of genes than CB1809-LP/CB1809-SP (1823 vs. 645 genes), with most of the transcripts being preferentially reduced (1156 vs. 382, respectively) under sub-optimal Pi conditions (Supplementary Figs. S2 and S3). The classification of the annotated DEGs into functional categories indicated that many genes were related to the primary (e.g., amino acid metabolism, protein, redox and transport) and secondary metabolism (e.g., phenylpropanoids and alkaloids) (Supplementary Fig. S5). Presumably, the downregulation of more genes in USDA110-LP/USDA110-SP was crucial for LP tolerance in USDA110-induced nodules. However, the expression changes in more genes in USDA110-LP/USDA110-SP might negatively affect the nodule adenylate pool and Pi reservoir under these conditions (Sulieman et al., 2022). The visualization by Venn diagram analysis further supports the differential transcriptional changes upon Pi scarcity in nodules inoculated with either USDA110 or CB1809 (Supplementary Fig. S6). In particular, there were 597 and 193 genes upregulated and downregulated, respectively, only in the USDA110-LP/USDA110-SP comparison, while there were 971 and 197 genes upregulated and downregulated, respectively, only in the CB1809-LP/CB1809-SP comparison (Supplementary Fig. S6; Supplementary Table S5A-B). Specifically, 70 (15%) and 185 (24%) of the upregulated and downregulated genes, respectively, obtained from comparisons USDA110-LP/USDA110-SP and CB1809-LP/CB1809-SP were overlapping (Supplementary Fig. S6; Supplementary Table S5A-B). On the other hand, 149 (33%) and 0 genes were upregulated, while 296 (67%) vs. 7 (100%) genes were downregulated in CB1809-SP/USDA110-SP vs. CB1809-LP/USDA110-LP, respectively (Supplementary Fig. S3; Supplementary Table S6A-C). This result indicates that USDA110 and CB1809 have differential effects on gene expression in soybean nodules under SP conditions rather than under LP conditions. Accordingly, no overlap occurred among the upregulated and downregulated genes obtained from comparisons CB1809-SP/USDA110-SP and CB1809-LP/USDA110-LP (Supplementary Fig. S6).

KEGG enrichment analysis of the unique DEGs in USDA110-LP/USDA110-SP and CB1809-LP/CB1809-SP comparisons indicated differential gene enrichment in different metabolic pathways between the two DEG sets (Supplementary Figs. S7 and S8). For instance, the unique, upregulated genes from the USDA110-LP/USDA110-SP were predominantly enriched in 'monobactam biosynthesis', 'sulfur metabolism', and 'riboflavin metabolism' pathways (Supplementary Fig. S7). However, the unique, upregulated genes from the CB1809-LP/CB1809-SP were notably enriched in 'limonene and pinene degradation', 'fatty acid biosynthesis' and 'fatty acid metabolism' pathways (Supplementary Fig. S7). On the other hand, the unique, downregulated genes from the USDA110-LP/USDA110-SP were predominantly enriched in 'stilbenoid diarylheptanoid and gingerol biosynthesis', 'flavonoid biosynthesis' and 'ABC transporters' pathways based on the KEGG enrichment analysis (Supplementary Fig. S8), while those from CB1809-LP/CB1809-SP were enriched in 'purine metabolism' and 'starch and sucrose metabolism' pathways (Supplementary Fig. S8). Furthermore, PPI network analysis showed that the unique, upregulated genes from the USDA110-LP/USDA110-SP exhibited predominant enrichment in 'threonine biosynthesis process', 'alanine-glyoxylate transaminase' and 'riboflavin metabolic process' (Supplementary Fig. S7), while those from the CB1809-LP/CB1809-SP were enriched in 'fatty acid β-oxidation' and 'electron transfer flavoprotein complex' pathways (Supplementary Fig. S7). Additionally, PPI analysis indicated that the unique, downregulated genes from the USDA110-LP/USDA110-SP showed significant enrichment in 'DNA replication', 'phenylpropanoid biosynthesis', 'flavonoid biosynthesis' and 'stilbenoid diarylheptanoid and gingerol biosynthesis' (Supplementary Fig. S8), while those from the CB1809-LP/CB1809-SP were enriched in 'purine metabolism' and 'starch and sucrose metabolism' pathways (Supplementary Fig. S8).

In addition, we successfully identified a total of 360 TF-encoding DEGs in USDA110-LP/USDA110-SP and CB1809-LP/CB1809-SP comparisons. These TFs showed regulatory interactions with 1823 DEGs in the USDA110-LP/USDA110-SP comparison and with 645 DEGs in the CB1809-LP/CB1809-SP comparison. Among the identified 360 TFs, 80 TFs in the USDA110-LP/USDA110-SP comparison and 66 TFs in the CB1809-LP/CB1809-SP comparison were found to have significantly overrepresented targets in identified DEGs (Supplementary Fig. S9). The 80 TFs were significantly (FDR < 0.05) enriched in C2C2 (Zn) DNA-binding with one zinc finger proteins [C2C2 (Zn) DOF], myeloblastosis/homeodomain-like (MYB/HD-like), no apical meristem/*Arabidopsis* transcription activation factor 1 and 2/cup-shaped cotyledon (NAC) and basic helix loop-helix (bHLH) TF family members (Supplementary Fig. S9). However, the 66 TFs were significantly enriched in teosinte branched 1, cycloidea, PCF (TCP), basic-leucine zipper (bZIP), SQUAMOSA promoter binding protein (SBP) and MYB/HD-like TF family members (Supplementary Fig. S9).

3.2. LP differentially orchestrates the C flux and turnover in nodules

The growth and nodulation of soybean are susceptible to Pi scarcity (Liu et al., 2018; Chen et al., 2019). This sensitivity is mainly ascribed to the substantial amount of Pi-dependent carbon (C) and energy turnover needed to sustain the function of bacteroids (~ 12.2 g C per g fixed N) (Streeter, 1991; Vance and Heichel, 1991; Zhang et al., 2020). As a result, the symbiotic nodule represents a large sink of photosynthates (~ 40% of photosynthetic C), which is required to sustain nodule respiration and subsequent metabolic activities (Vauclare et al., 2010). Unfortunately, the nodule C-cost penalty increases in soybean exposed to Pi deficiency (Le Roux et al., 2009). Thus, multifaceted adjustments in nodule C metabolism must be strictly regulated to avoid photoassimilates' overexploitation, while permitting the rest of metabolic functions (Sulieman et al., 2022 and references therein).

3.2.1. Sucrose cleavage and phosphorylation of hexoses

Phloem-imported carbohydrates (i.e., sucrose) ultimately synthesized in the aerial parts are the preferential forms of C assimilates processed to power the operation of nodule symbiosis (Streeter, 1991; Oehrle et al., 2008; Zhang et al., 2020). Our recently documented metabolome profiling demonstrated that the W82 nodules were not deprived of photoassimilates during Pi limitation (Sulieman et al., 2019). This finding was supported by the fairly stable levels of sucrose and other derived sugars under the experimental conditions similar to those used in the present study. Sucrose is the preferential form of C fluxed to power the nodule respiratory metabolism (Day and Copeland, 1991; Gordon et al., 1999). Before utilization, sucrose must be first degraded into hexoses by the specific action of sucrose synthase (SUS) and/or invertase (Fig. 1). There is a consensus that SUS is the main enzyme implicated in sucrose hydrolysis, which is essential for soybean N_2 fixation (Anthon and Emerich, 1990; Gordon et al., 1999; Lyu et al., 2022). While a putative invertase gene (*Glyma.10G214700*) with a downregulated expression level (by 2.37-fold) was detected in CB1809-LP/CB1809-SP, the expression of the *Glyma.09G073600* and *Glyma.15G182600* genes, encoding SUS4 enzymes, and the expression of the *Glyma.04G005700* gene, putatively encoding invertase, were upregulated by 7.65-, 7.52- and 2.07-fold, respectively, in the USDA110-LP/USDA110-SP comparison (Fig. 1). Our findings suggest

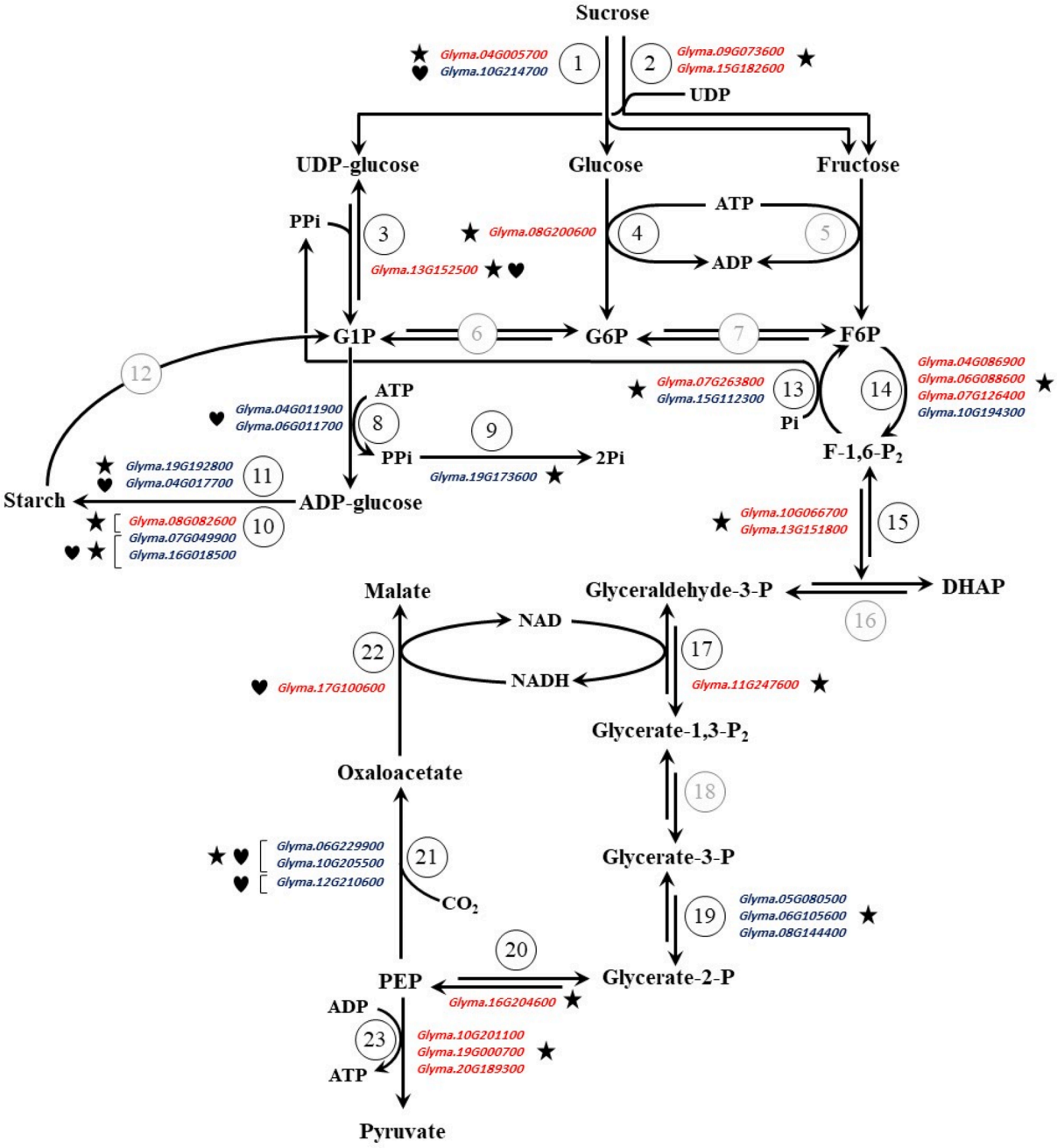

Fig. 1. The expression patterns of genes encoding enzymes implicated in sucrose breakdown and glycolysis in the nodules of soybean (cv. Williams 82) inoculated with *Bradyrhizobium diazoefficiens* USDA110 or CB1809 and subjected to low (0.1 mM; LP) or sufficient (2.0 mM; SP) phosphate levels. Black stars denote USDA110-LP/USDA110-SP comparison, while black hearts indicate CB1809-LP/CB1809-SP comparison. Red and blue colors represent upregulated and downregulated genes (fold-change ≥ 2 and ≤ -2; q-value < 0.05), respectively. The numbers displayed in the scheme refer to the following enzymes: (1) invertase, (2) sucrose synthase, (3) UDP-glucose pyrophosphorylase, (4) hexokinase, (5) fruktokinase, (6) phosphoglucomutase, (7) phosphohexose isomerase, (8) ADP-glucose pyrophosphorylase, (9) pyrophosphatase, (10) starch synthase, (11) starch-branching enzyme, (12) starch phosphorylase, (13) phosphofructophosphotransferase, (14) phosphofructokinase, (15) fructose-1,6-bisphosphate aldolase, (16) triose phosphate isomerase, (17) glyceraldehyde-3-phosphate dehydrogenase, (18) phosphoglycerate kinase, (19) phosphoglycerate mutase, (20) enolase, (21) phosphoenolpyruvate carboxylase, (22) malate dehydrogenase, (23) pyruvate kinase. Grey numbers denote non-differentially expressed genes (no change). Abbreviations: DHAP, dihydroxyacetone phosphate; F-1,6-P_2, fructose-1,6-bisphosphate; F6P, fructose-6-phosphate; glycerate-1,3-P_2, glycerate-1,3-biphosphate; glycerate-2-P, glycerate 2 phosphate; glyceraldehyde-3-P, glycerate-3-phosphate; G1P, glucose-1-phosphate; G6P, glucose-6-phosphate; PEP, phosphoenolpyruvate; Pi, inorganic phosphate; PPi, pyrophosphate; UDP, uridine diphosphate.

that both catabolic routes were active in the Pi-deprived nodules, with an enhanced potential need for sucrose breakdown in the nodules colonized by the USDA110 strain. However, the invertase catabolic route is energetically costlier than the SUS route (4:3 ATPs for invertase/SUS routes in transforming sucrose to triose-Pi, respectively) (Oehrle et al., 2008). Some published reports found that the invertase route consumes double the amount of ATPs used to convert sucrose to fructose-6-phosphate via the SUS pathway (Dennis and Greyson, 1987; Rychter and Szal, 2015), making invertase a futile route during Pi deficiency.

As suspected, the *Glyma.13G152500* gene, putatively encoding a pyrophosphate (PPi)-dependent UDP–glucose pyrophosphorylase

(UGPase), exhibited strong upregulation by 5.83- and 7.16-fold in CB1809-LP/CB1809-SP and USDA110-LP/USDA110-SP, respectively (Fig. 1). This ATP-conserving protein represents a valuable facet of acclimatization, which can use PPi as an alternate phosphoryl source, presumably to preserve the limited pool of cellular adenylates during Pi scarcity (Le Roux et al., 2009; Nasr Esfahani et al., 2016; Li et al., 2022) (Fig. 1). Simultaneously, Pi liberated via these PPi-dependent metabolic routes can be reused to facilitate other functions in the nodules undergoing Pi starvation. One gene (*Glyma.08G182300*) putatively encoding fructose-1,6-bisphosphatase was upregulated by 2.50-fold in the CB1809-LP/CB1809-SP comparison only. The LP-inducible transcription patterns observed across the nodular cortical zone for an orthologous gene in common bean (*Phaseolus vulgaris*) were found to be closely associated with efficient Pi remobilization and beneficial impacts on nodule tolerance to Pi deficiency (Lazali et al., 2016). The vital roles of this regulatory gene have been demonstrated in nodule-Pi homeostasis and the control of O_2 permeability in the nodules of Pi-starved common bean (Lazali et al., 2016).

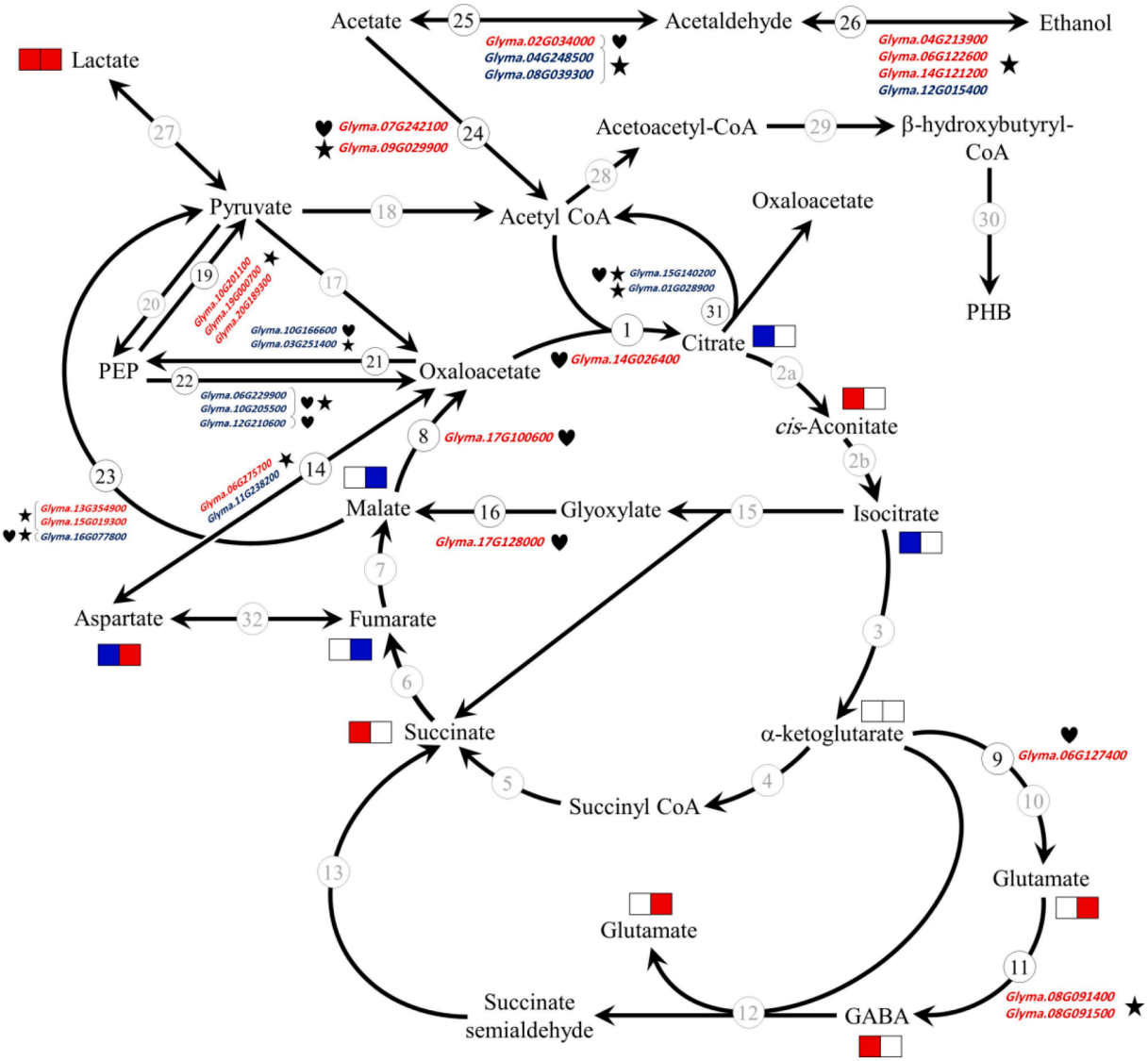

Fig. 2. The expression patterns of genes encoding enzymes implicated in the Krebs cycle and associated carbon metabolic pathways in the nodules of soybean (cv. Williams 82) inoculated with *Bradyrhizobium diazoefficiens* USDA110 or CB1809 and subjected to low (0.1 mM; LP) or sufficient (2.0 mM; SP) phosphate levels. Black stars denote USDA110-LP/USDA110-SP comparison, while black hearts indicate CB1809-LP/CB1809-SP comparison. Red and blue colors represent upregulated and downregulated genes (fold-change ≥ 2 and ≤ -2; q-value < 0.05), respectively. The concentrations of metabolites were retrieved from Sulieman et al. (2019). Blue-, red- and white-colored squares denote increases, decreases and unaltered amounts of metabolites, respectively, in LP-treated nodules vs. SP-treated nodules. The left and right squares refer to the USDA110- and CB1809-colonized nodules, respectively. The numbers displayed in the scheme indicate the following enzymes related to various nodule carbon metabolic pathways: (1) citrate synthase, (2) aconitase, (3) isocitrate dehydrogenase, (4) α-ketoglutarate dehydrogenase, (5) succinyl-CoA synthetase, (6) succinate dehydrogenase, (7) fumarase, (8) malate dehydrogenase, (9), glutamate synthase, (10) glutamate dehydrogenase, (11) glutamate decarboxylase, (12) γ-aminobutyrate aminotransferase, (13) succinate semialdehyde dehydrogenase, (14) aspartate aminotransferase, (15) isocitrate lyase, (16) malate synthase, (17) pyruvate carboxylase, (18) pyruvate dehydrogenase complex, (19) pyruvate kinase, (20) pyruvate orthophosphate dikinase, (21) phosphoenolpyruvate carboxykinase, (22) phosphoenolpyruvate carboxylase, (23) NAD(P) malic enzyme, (24) acetate-CoA ligase, (25) aldehyde dehydrogenase, (26) alcohol dehydrogenase, (27) lactate dehydrogenase, (28) β-ketothiolase, (29) β-hydroxybutyryl-CoA reductase, (30) poly-β-hydroxybutyrate polymerase, (31) citrate lyase, (32) aspartase. Grey numbers denote non-differentially expressed genes (no change). Abbreviations: GABA, γ-aminobutyric acid; PEP, phosphoenolpyruvate; PHB, poly-β-hydroxybutyrate.

3.2.2. Glycolytic route and alternative energy-saving pathways

The transcript abundance of several genes encoding enzymes implicated in the glycolytic shunt was significantly increased in responses to Pi deficiency, especially in the USDA110-LP/USDA110-SP comparison (Fig. 1). Of particular interest in this context was the upregulation of multiple genes encoding ATP-binding hexokinase (*Glyma.08G200600/HXK1*), putative phosphofructophosphotransferase (*Glyma.07G263800*), phosphofructokinase (PFK) family proteins (3 genes: *Glyma.04G086900, Glyma.06G088600* and *Glyma.07G126400*), putative fructose-1,6-bisphosphate aldolases (2 genes: *Glyma.10G066700* and *Glyma.13G151800*), phosphorylating NAD^+-dependent glyceraldehyde-3-phosphate dehydrogenase (*Glyma.11G247600/GAPC*), enolase (*Glyma.16G204600*) and PKs (3 genes: *Glyma.10G201100, Glyma.19G000700* and *Glyma.20G189300*) in USDA110-LP/USDA110-SP (Fig. 1). The activities of some corresponding enzymes (e.g., PFK, HXK, GAPC and PK) are regulated by Pi and cellular concentrations of adenylates (Rychter and Szal, 2015). Not surprisingly, PFK proteins are crucial to fine-tuning the glycolytic pathway, whereas HXK enzymes integrate the C/N signals and controls metabolic activities (Vance, 2008). On the other hand, GAPC is a multifunctional enzyme that could play vital functions in glycolysis and gluconeogenesis (Zeng et al., 2016). In addition to the respiratory flux, it was revealed that GAPC has numerous cellular functions, especially in responses to environmental stimuli. Nevertheless, we observed lower transcript abundance of some genes encoding PFK-family protein (*Glyma.10G194300*), putative phosphofructophosphotransferase (*Glyma.15G112300*) and phosphoglycerate mutases (3 genes: *Glyma.05G080500, Glyma.06G105600* and *Glyma.08G144400*) in the USDA110-LP/USDA110-SP comparison only (Fig. 1).

The low cellular concentrations of Pi and adenylate pools in Pi-deprived plants could negatively affect the activities of some classical enzymes engaged in the glycolytic pathway (Juszczuk and Rychter, 2002; Li et al., 2022). Since ADP could drastically reduce PK activities upon Pi starvation, it was likely that the Pi-starved soybean nodules would bypass this reaction through an alternative energy-saving pathway that comprises phosphoenolpyruvate carboxylases (PEPC) (Figs. 1 and 2). These responses would likely maintain energy consumption despite the sharp reduction in nodule-Pi pool under Pi deficiency (Sulieman et al., 2022). Nevertheless, this was not the case in nodules of both *B. diazoefficiens*-soybean combinations, especially in the case of USDA110, where three genes (*Glyma.10G201100, Glyma.19G000700* and *Glyma.20G189300*) putatively encoding PKs were upregulated in USDA110-LP/USDA110-SP (Figs. 1 and 2). The conceptual illustrations in Figs. 1 and 2 demonstrated that the final glycolytic products are determined by the potential catalytic action of either PKs or PEPCs (Day and Copeland, 1991; Sulieman et al., 2022). This work and other reports therefore suggest that PEPCs might contribute more than PKs in facilitating phosphoenolpyruvate (PEP) carboxylation under low Pi availability (Figs. 1 and 2). It has been well established that soybean functional nodules contain several genes encoding PEPC isoenzymes (0.5–2.0% of the total soluble proteins) (Deroche and Carrayol, 1988). Here, we detected the downregulated expression of the *Glyma.06G229900* gene encoding PEPC3 (by 3.82- and 3.16-fold) and the *Glyma.10G205500* gene encoding PEPC4 (by 9.51- and 3.05-fold) in CB1809-LP/CB1809-SP and USDA110-LP/USDA110-SP, respectively (Figs. 1 and 2). In addition, one gene (*Glyma.12G210600*) encoding PEPC3 was downregulated by 2.24-fold in CB1809-LP/CB1809-SP but not in USDA110-LP/USDA110-SP (Figs. 1 and 2). Likewise, the transcript abundance of the *Glyma.10G166600* and *Glyma.03G251400* genes encoding phosphoenolpyruvate carboxykinase 1 (PPCK1) involved in the phosphorylation of PEPC (Vidal and Chollet, 1997) was reduced by 3.52- and 4.55-fold in CB1809-LP/CB1809-SP and USDA110-LP/USDA110-SP, respectively (Fig. 2). These findings were surprising because it is widely believed that PEPCs contribute substantially to the nodule C budget by re-fixing CO_2, and thus, compensating a part of the nodule C respired (~14% in ureide-exporting nodules) (Streeter, 1991). However, it has been previously noticed that a sharp reduction in CO_2 fixation occurred in soybean nodules together with the lower nitrogenase activity (measured with C_2H_2 reduction assay) at a point of time when ureides formation and export increased at the expense of amino acids, notably asparagine (Coker and Schubert, 1981).

A considerable impact on other candidate genes engaged in CO_2 cycling (Wang et al., 2021) was also evident in the Pi-starved USDA110 nodules. This response includes the downregulation of the *Glyma.19G135900* and *Glyma.19G185900* genes encoding carbonic anhydrase (CA) family proteins and the *Glyma.06G182700* gene encoding β-CA2 by 2.12-, 4.37- and 4.94-fold, respectively, in the USDA110-LP/USDA110-SP comparison only. The notable exception was the upregulation of the *Glyma.11G196700* gene encoding a CA-family protein by 2.03-fold in the same *B. diazoefficiens* comparison. Based on the specific gene expression localization in the nodule cortex, it has been postulated that CA might be implicated in the putative gaseous (O_2/CO_2 exchange) control and organic acid (malate) generation (Atkins et al., 2001; Vance, 2008; Wang et al., 2021). However, not all researchers agreed with the relative importance of CO_2 fixation in nodule metabolism (Verma, 1989; Streeter, 1991). For instance, it has been argued that the dark fixation of CO_2 is an energy-requiring process, which unlikely provides remarkable rewards to the overall nodule C budget (Streeter, 1991).

3.2.3. Malate metabolism in nodule symbiosome

Regulation of C4-dicarboxylate metabolism is vital to efficient symbiosis under LP availability (Zhu et al., 2021; Lyu et al., 2022). Our results detected an upregulation of the *Glyma.17G100600* gene encoding malate dehydrogenase (MDH) (by 2.11-fold) in CB1809-LP/CB1809-SP but not in USDA110-LP/USDA110-SP (Figs. 1 and 2). This ubiquitous enzyme is responsible for the reversible conversion of oxaloacetate to malate (Zhu et al., 2021), which can promote the acclimatization of CB1809 nodules under Pi deficiency (Sulieman et al., 2019). This finding concurs with our metabolome profiling that recorded higher malate levels in the Pi-starved CB1809 nodules than in the USDA110 nodules (Fig. 2). Subsequently, malate derived from oxaloacetate could be channeled into the bacteroids and used as a preferential respiratory substrate for nitrogenase activity (Booth et al., 2021; Sulieman et al., 2022). Apart from MDH-encoding *Glyma.17G100600* gene, other DEGs involved in malate synthesis were observed in the Pi-starved W82 nodules. Notably, the transcript abundance of the *Glyma.17G128000* gene encoding malate synthase (MLS) was upregulated by 2.90-fold in CB1809-LP/CB1809-SP only (Fig. 2). This key peroxisomal enzyme is responsible for the condensation of acetyl-coenzyme A (acetyl-CoA) and glyoxylate in the final metabolic reaction of the glyoxylate shunt, hence anaplerotic replenishing the pool size of the Krebs cycle intermediates (García-de los Santos et al., 2002) (Fig. 2). Some researchers have drawn attention to the fact that a large proportion of acetyl-CoA (~50%) directed to the Krebs cycle was catabolized in soybean nodules through the MLS-metabolic pathway and that the bacteroids isolated from soybean nodules displayed higher MLS activities compared with those isolated from amide-producing nodules (McDermott et al., 1989; Green et al., 1998). To this end, the glyoxylate bypass might help to reallocate C from other sources (i.e., structural lipids/fatty acids) during nodular senescence or low respiratory quotients (Fargeix et al., 2004). Thus, it can be expected that other genes dedicated to malate biosynthesis and not a part of the mitochondrial Krebs cycle might be additionally expressed during Pi deprivation (Fig. 2). Given the vital role of malate in symbiotic efficiency, the induction of the MLS-encoding *Glyma.17G128000* gene in response to Pi deficiency is an intriguing finding that opens up a new question for further studies.

In N_2-fixing bacteroids, malate could be oxidatively decarboxylated to pyruvate, which in turn could be converted to acetyl-CoA and consequently channeled into the Krebs cycle for energy production (Booth et al., 2021) (Fig. 2). The metabolism of malate is usually

achieved via the catalytic actions of MDH (to oxaloacetate) and malic enzyme (ME), which has two distinct metabolic forms based on the specific substrate used as a cofactor: NAD^+-linked ME (DME) and $NADP^+$-linked ME (TME) (Liu et al., 2018) (Fig. 2). It has previously been demonstrated that soybean bacteroids comprise both forms of ME, with the DME being only functionally essential for nitrogenase activity (Day and Copeland, 1991; Booth et al., 2021). In this context, the *Glyma.16G077800* gene encoding TME4 was downregulated by 3.04- and 2.64-fold in CB1809-LP/CB1809-SP and USDA110-LP/USDA110-SP, respectively (Fig. 2). The repression of the gene encoding TME4 might indicate that DME was actively involved in malate decarboxylation in nodules of both *B. diazoefficiens*-soybean combinations. It has been previously noted that DME is among the vital bypasses employed to eliminate the adenylate and Pi-dependent biochemical reactions in *Brassica nigra* in response to Pi limitation (Rychter and Szal, 2015). However, the transcript levels of the *Glyma.13G354900* and *Glyma.15G019300* genes encoding TME4 were increased (by 2.45- and 2.46-fold, respectively) in USDA110-LP/USDA110-SP but not in CB1809-LP/CB1809-SP (Fig. 2). Several research groups suggested that the constitutive TME enzyme is involved in biosynthetic and maintenance activities rather than catabolic functions in N_2-fixing bacteroids (Copeland et al., 1989; Day and Copeland, 1991; Driscoll and Finan, 1996). This premise was supported by the higher affinity (K_m) and the lower TME activity level for malate than those of DME in functional bacteroids (Copeland et al., 1989; Driscoll and Finan, 1996). Despite these results, we cannot rule out that TME might have a catalytic efficiency for malate oxidation, especially under lower malate concentrations observed in Pi-starved USDA110-nodules (Sulieman et al., 2019). From the preceding discussion, it is likely that CB1809-nodules possessed a relatively more vital catabolic ability for higher demand of malate by upregulating an MDH gene (*Glyma.17G100600*) and reducing a TME4 gene (*Glyma.16G077800*) for efficient energy generation under Pi deficiency (Fig. 2). We encourage further research to dissect the precise functional roles of TME4-encoding genes in Pi-stressed soybean nodules.

3.2.4. *Mitochondrial respiratory chain*

In addition to glycolysis and the Krebs cycle, our present results revealed that the mitochondrial electron transport chain (mETC) was differentially affected in nodules of both *B. diazoefficiens*-soybean combinations at the transcriptional level. Based on the present analysis, the expression level of the *Glyma.10G012800* gene encoding cytochrome c oxidase subunit Vc (COX5C) involved in the conventional electron transport machinery (Gupta et al., 2015) was putatively upregulated by 2.35-fold in USDA110-LP/USDA110-SP only (Fig. 3). This response likely ensured the high energy required to support the extensive metabolic adjustments employed by USDA110-nodules under Pi deficiency (Supplementary Figs. S2 and S3). However, the cytochrome chain is an energy-demanding route that could increase oxidative stress under Pi deficiency (Rychter and Szal, 2015). This circumstance might explain the downregulation of the *Glyma.09G196400* gene, encoding F1-ATPase engaged in ATP generation (Prasad and Stewart, 1992), by 2.69-fold in

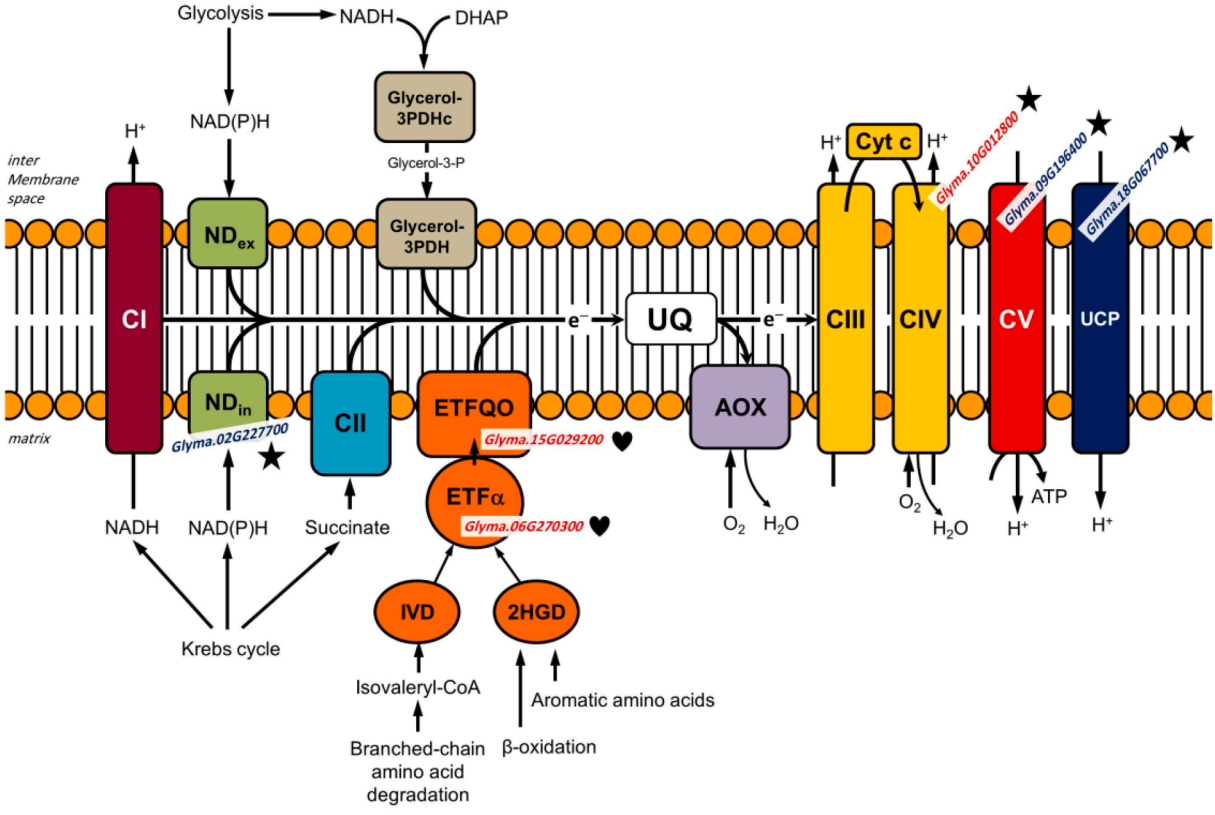

Fig. 3. The expression patterns of genes encoding enzymes implicated in mitochondrial oxidative phosphorylation in the nodules of soybean (cv. Williams 82) inoculated with *Bradyrhizobium diazoefficiens* USDA110 or CB1809 and subjected to low (0.1 mM; LP) or sufficient (2.0 mM; SP) phosphate levels. Black stars denote USDA110-LP/USDA110-SP comparison, while black hearts indicate CB1809-LP/CB1809-SP comparison. Red and blue colors represent upregulated and downregulated genes (fold-change ≥ 2 and ≤ -2; q-value < 0.05), respectively. Abbreviations: 2HGD, 2-hydroxyglutarate dehydrogenase; AOX, alternative oxidase; CI, NADH dehydrogenase; CII, succinate dehydrogenase; CIII, cytochrome c reductase; CIV, cytochrome c oxidase; CV, ATP synthase; cyt c, cytochrome c; DHAP, dihydroxyacetone phosphate; *e*−, electron flux; ETF, electron transfer flavoprotein; ETFQO, electron transfer flavoprotein quinine oxidoreductase; Glycerol-3-P, glycerol-3-phosphate; Glycerol-3PDH, glycerol-3-phosphate dehydrogenase; Glycerol-3PDHc, cytosolic glycerol-3-phosphate dehydrogenase; IVD, isovaleryl-CoA dehydrogenase; ND_{ex}, external type II NAD(P)H dehydrogenase; ND_{in}, internal type II NAD(P)H dehydrogenase; UCP, plant uncoupling protein; UQ, ubiquinone pool. Figure redrawn from Møller et al. (2021).

the USDA110-nodules (Fig. 3). The use of the cytochrome pathway in USDA110-nodules under Pi deficiency was supported by the lower transcript levels of some genes engaged in non-phosphorylating bypasses (Fig. 3). Of particular interest here was the downregulation of the *Glyma.02G227700* and *Glyma.18G067700* encoding alternative internal NAD(P)H type II dehydrogenase 1 (NDI1) and uncoupling protein 2 (UCP2) (Gupta et al., 2015) by 2.88- and 2.01-fold, respectively, in USDA110-LP/USDA110-SP only (Fig. 3). In contrast, the CB1809-LP/CB1809-SP showed the induction of two genes involved in an energy-saving bypass (Gupta et al., 2015) (Fig. 3). Specifically, the transcript levels of *Glyma.06G270300* and *Glyma.15G029200* genes, encoding FAD-binding electron transfer flavoprotein alpha (ETFα) and flavoprotein:ubiqionone oxidoreductase (ETFQO), respectively (Gupta et al., 2015), were increased by 2.13- and 2.43-fold, respectively, in CB1809-LP/CB1809-SP but not USDA110-LP/USDA110-SP (Fig. 3). Under LP conditions, the higher capacity of EFT was probably essential for the electron flow to the ubiquinone (UQ) via the membrane-bound ETFQO, thereby bypassing the phosphorylation sites at the main respiratory chain, which in turn could suppress the respiration-induced oxidative stress in CB1809-nodules under Pi deficiency (Gupta et al., 2015).

3.3. Inductions of other alternative C flux strategies in Pi-deprived nodules

3.3.1. Alcoholic fermentation pathway

The present results suggest that USDA110-nodules activated some alternate drastic metabolic pathways that might go hand-in-hand with the above-mentioned metabolic acclimatization under Pi deficiency. For instance, our results indicated that USDA110-nodules were likely to enhance the fermentation metabolism during LP stress (Fig. 4). In support of this, it has previously been found that the fermentation pathway was actively involved in soybean nodules during normal or stress (e.g., waterlogging) conditions (Tajima and Larue, 1982; Suganuma and Yamamoto, 1987; Borella et al., 2014). This acclimatization response was supported by the solid higher abundance of the *Glyma.01G118000* and *Glyma.03G055100* transcripts, putatively coding for pyruvate decarboxylase 2 (PDC2) enzymes, in USDA110-LP/USDA110-SP by 41.44- and 14.98-fold, respectively (Fig. 4). In the same vein, we observed the upregulated expression of the *Glyma.04G213900, Glyma.06G122600* and *Glyma.14G121200* encoding alcohol dehydrogenase 1 (ADH1) enzymes by 3.98-, 2.46- and 5.75-fold, respectively, in the same USDA110-LP/USDA110-SP (Figs. 2 and 4). In the same comparison, an only exception was found, which was the downregulated expression of the *Glyma.12G015400* gene (by 2.49-fold), putatively encoding ADH (Figs. 2 and 4). The increased flow of C derived from glycolysis into the ethanolic fermentation at the expense of mitochondrial respiration might help the continuation of ATP biosynthesis, while concomitantly ensuring the NAD^+ recycling via NADH oxidation, which is indispensable to avoid diminishing the glycolytic flux, especially when oxidative phosphorylation is profoundly hindered (Juszczuk and Rychter, 2002; Zabalza et al., 2009). Accordingly, it can be suggested that the activation of the fermentation pathway was closely related to the energy state of nodules and not exclusively relied on the O_2 availability. Furthermore, consuming protons associated with substrate-level energy generation was essential to reduce the cytosolic acidification that often occurs during fermentation (Gout et al., 2001; Borella et al., 2014). Despite these results, the accumulation of the fermentative product, namely acetaldehyde, was found to be potentially cytotoxic if produced in higher concentrations that might induce protein adducts (Ricoult

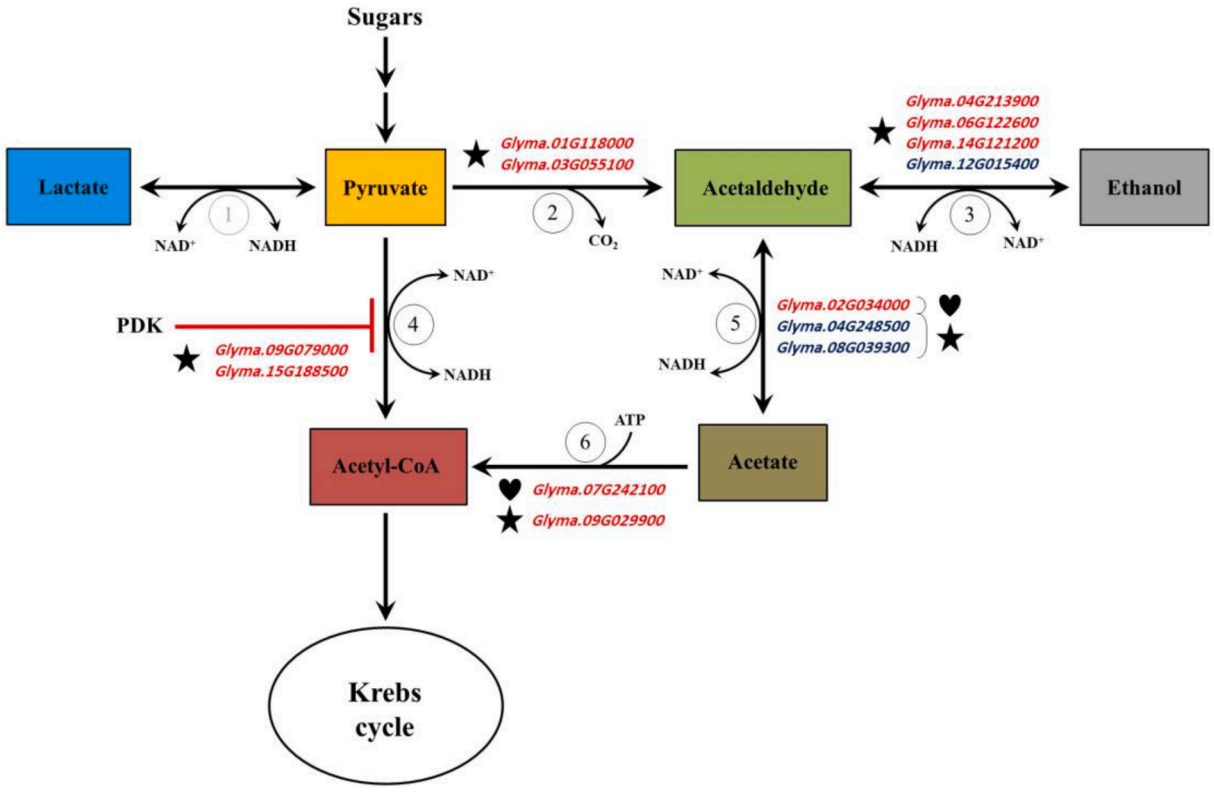

Fig. 4. Expression pattern of genes encoding enzymes implicated in ethanolic fermentation and associated carbon metabolic pathways in the nodules of soybean (cv. Williams 82) inoculated with *Bradyrhizobium diazoefficiens* USDA110 or CB1809 and subjected to low (0.1 mM; LP) or sufficient (2.0 mM; SP) phosphate levels. Black stars denote USDA110-LP/USDA110-SP comparison, while black hearts indicate CB1809-LP/CB1809-SP comparison. Red and blue colors represent upregulated and downregulated genes (fold-change ≥ 2 and ≤ -2; q-value < 0.05), respectively. Red bar denotes inhibition. The numbers displayed in the scheme refer to the following enzymes: (1) lactate dehydrogenase, (2) pyruvate decarboxylase, (3) alcohol dehydrogenase, (4) pyruvate dehydrogenase complex, (5) aldehyde dehydrogenase, (6) acetate-CoA ligase. Grey numbers denote non-differentially expressed genes (no change). Abbreviations: PDK, pyruvate dehydrogenase kinase.

et al., 2005). Moreover, ethanol is a dead-end product, which might be diffused out of the nodules, leading to C loss, especially under low carbohydrate conditions (Ricoult et al., 2005; Borella et al., 2014; da-Silva and do Amarante, 2020).

In order to direct the C flux into the fermentation metabolism, the expression levels of two genes (*Glyma.09G079000* and *Glyma.15G188500*), encoding ATP-binding pyruvate dehydrogenase kinases (PDKs), were increased by 2.48- and 2.46-fold, respectively, whereas the coordinated expression of the *Glyma.04G248500/ALDH4* and *Glyma.08G039300/ALDH1A* genes encoding aldehyde dehydrogenases (ALDHs) was downregulated by 2.56- and 2.65-fold, respectively, in USDA110-nodules by Pi deficiency (Figs. 2 and 4). Contrarily, we detected upregulated expression of the *Glyma.02G034000* gene only, which encodes ALDH2B7, by 4.64-fold in the CB1809-LP/CB1809-SP comparison (Figs. 2 and 4). For Pi-starved USDA110-nodules, the upregulation of the *PDK* genes could help suppress the pyruvate dehydrogenase complex (PDH), and consequently, the acetyl-CoA provision into the Krebs cycle (Marillia et al., 2003) (Fig. 4). PDC is, thus, a critical metabolic node that could regulate the C-metabolic traffic into the mitochondrial metabolism (i.e., Krebs cycle) for the maintenance of respiration (Weraduwage et al., 2016) under LP conditions (Fig. 4). Apart from PDC, ALDH could be involved in other metabolic pathways (Tola et al., 2021). For instance, it has been found that ALDH was strongly implicated in the conversion of $NAD(P)^+$ into NAD(P)H (Kotchoni et al., 2006), thereby likely contributing to energy production and respiratory homeostasis in the Pi-starved CB1809-nodules. As previously reported in soybean, isolated bacteroids successfully used acetaldehyde as a C substrate for N_2 fixation (Tajima and Larue, 1982; Suganuma and Yamamoto, 1987). The possible use of acetaldehyde as a C substrate for N_2 fixation could be supported by the higher expression levels of the *Glyma.09G029900* and *Glyma.07G242100* genes, encoding AMP binding-acetate-CoA ligase (AAE7/ACN1) involved in the oxidation of acetate, i.e., PDH bypass (Oliver et al., 2009; Zhao et al., 2021), by 14.56-fold and 2.68-fold in the USDA110-LP/USDA110-SP and CB1809-LP/CB1809-SP comparisons, respectively (Figs. 2 and 4).

3.3.2. γ-Aminobutyrate (GABA) shunt

Another metabolic bypass that might be involved in promoting the acclimatization of nodules under Pi deficiency is the "GABA shunt" (Sulieman and Schulze, 2010; Nasr Esfahani et al., 2016). This metabolic bypass represents the primary route for GABA biosynthesis via the catalytic action of glutamate decarboxylase (GAD) (Souza et al., 2016; Shelp et al., 2017) (Fig. 2). By circumventing the stress-sensitive reactions of the Krebs cycle (α-ketoglutarate-to-succinate) for the maintenance of respiration (Fig. 2), it becomes evident that this conserved metabolic pathway could profoundly contribute to the C/N homeostasis and nodule functioning, especially during stressful conditions (Sulieman and Schulze, 2010; Souza et al., 2016). Our transcriptome analysis revealed an upregulation of the *Glyma.08G091400* and *Glyma.08G091500* genes encoding calmodulin-binding GAD1 enzymes by 8.80- and 4.63-fold, respectively, in the USDA110-LP/USDA110-SP comparison only (Fig. 2). The GAD metabolic activity is a proton-consuming (H^+ sink) reaction that appears preferentially favored under restricted O_2 conditions (Shelp et al., 2017). Thus, the induction of the GAD1-encoding genes during the cytosolic anaerobic conditions might help nodules reduce the cytosolic acidification (pH homeostasis), which likely occurs during Pi deficiency (Nasr Esfahani et al., 2016). The results suggest that soybean plants possess metabolic flexibility that might help nodules attenuate LP availability.

3.4. Transitory starch reserves can promote nodule tolerance to LP

Our gene expression analysis showed that numerous genes encoding proteins related to the synthesis and turnover of storage reserves were actively involved at transcriptional level during Pi starvation (Fig. 1). Starch is the main carbohydrate reservoir that could buffer sucrose fluctuation during the conditions that lead to excess or acute energy limitations in soybean nodules (Vance and Heichel, 1991; Georgiev and Tsvetkova, 2011; Zhang et al., 2020). Thus, it could be suggested that the CB1809-associated nodules blocked the pathways of starch biosynthesis to sustain the bacteroids' respiratory demand, thereby diverting the photoassimilate supply toward glycolysis and the Krebs cycle (Fig. 1). This response was evident by the intense repression of the *Glyma.04G011900* (by 14.05-fold) and *Glyma.06G011700* (by 11.92-fold) genes, encoding ADP-glucose pyrophosphorylase, the precursor that allosterically regulated starch biosynthesis in plants (Kolbe et al., 2005), in CB1809-LP/CB1809-SP (Fig. 1). In addition, the expression of the *Glyma.07G049900* and *Glyma.16G018500* genes putatively encoding starch synthase involved in starch biosynthesis (Baslam et al., 2021) was downregulated in both USDA110-LP/USDA110-SP (by 3.57- and 2.11-fold) and CB1809-LP/CB1809-SP (by 12.65- and 6.37-fold, respectively) (Fig. 1). The notable exception was the increased expression of the *Glyma.08G082600/SSIV* gene encoding starch synthase 4 in USDA110-LP/USDA110-SP (by 2.18-fold) but not in CB1809-LP/CB1809-SP (Fig. 1). Moreover, the transcript levels of the *Glyma.04G017700* and *Glyma.19G192800* genes encoding starch--branching enzyme 2.2 (SBE2.2), which additionally contributes to starch formation (Baslam et al., 2021) decreased by 3.99- and 3.19-fold in CB1809-LP/CB1809-SP and USDA110-LP/USDA110-SP, respectively (Fig. 1). Therefore, it could be assumed that the high potential respiratory demand coupled with the increased expression levels of the genes related to sucrose breakdown (i.e., invertase, SUS and UGPase) might coordinately contribute to exhausting the pool size of starch in the Pi-starved USDA110-nodules (Fig. 1). Under such conditions, the expression of genes, encoding α-amylase-like 2 (*Glyma.14G222600/-AMY2*) and β-amylase 3/8 (BMY8/BAM3) (*Glyma.05G068000* and *Glyma.17G150100*) coordinately engaged in starch breakdown (Baslam et al., 2021), was upregulated in USDA110-LP/USDA110-SP (by 2.31-, 6.84- and 2.69-fold, respectively) but not in CB1809-LP/CB1809-SP. The stability of maltose and sucrose, the main products of starch breakdown, in the Pi-starved USDA110 nodules (Sulieman et al., 2019) could partially support our results. Our findings might explain why previous studies have noticed sharp reductions in starch deposits when soybean nodules were exposed to Pi starvation (Ribet and Drevon, 1995; Georgiev and Tsvetkova, 2011).

3.5. An integrative view of nodule respiratory pathways under LP stress

Pi deficiency negatively affects the energy metabolism in the USDA110-nodules by interfering with the mitochondrial oxidative phosphorylation (i.e., F1-ATPase) (Fig. 3), more likely leading to lower ATP production, which could impair the nodulation and overall plant growth (Sulieman et al., 2019). It is tempting to suggest that the USDA110-inoculated plants responded to LP stress by adjusting the expression of genes regulating the respiratory metabolic pathways (Figs. 1, 2 and 4). To cope with energy limitation induced by LP availability, the Pi-deprived USDA110-nodules enhanced the expression of genes implicated in sucrose cleavage (i.e., those encoding SUS and invertase) and starch breakdown (i.e., those encoding AMY2 and BMY8/BAM3), while largely reducing the transcript levels of genes involved in starch formation (i.e., those encoding starch synthase and SBE2.2) (Fig. 1). Notably, the Pi-deprived USDA110-nodules strongly induced the expression of numerous genes related to glycolysis (i.e., those encoding HXK, phosphofructophosphotransferase, PFK, fructose-1,6-bisphosphate aldolases, GAPC, enolase and PK) and alcoholic fermentation (e.g., those encoding PDC2 and ADH1) pathways (Figs. 1, 2 and 4). This response could help NAD^+ recycling and accelerate ATP generation under LP availability (Juszczuk and Rychter, 2002). Additionally, the Pi-deprived USDA110-nodules induced the expression levels of GAD1-encoding genes implicated in GABA shunt, which might help reduce the cytosolic acidification and circumvent the

stress-sensitive reactions of the Krebs cycle for the maintenance of respiration (Sulieman and Schulze, 2010; Souza et al., 2016) (Fig. 2). Although the energy generated via these metabolic arrangements can partially alleviate the energy deficiency caused by inhibiting oxidative phosphorylation, such arrangements might be accompanied by higher C cost resulted from the upregulation of genes employed in numerous ATP-dependent respiratory pathways (e.g., those encoding HXK, PFK, GAPC and PK) and oxidative stress (e.g., encoding COX5C), which could disrupt cell homeostasis and eventually lead to lower symbiotic efficiency. In contrast, the Pi-deprived CB1809-nodules enhanced the transcript abundance of genes involved in non-phosphorylating bypass (e.g., those encoding ETFα and ETFQO) and induced the expression of genes engaged in malate formation (i.e., those encoding MDH and MLS) to power nitrogenase activity and subsequent N assimilation. Collectively, the relatively lower number of genes regulated in the Pi-starved CB1809-nodules was anticipated to reduce the overall metabolic C cost, leading to less sensitivity to Pi stress.

4. Concluding remarks

Soybean (W82) acclimatization to Pi starvation strongly depends on the *Bradyrhizobium* strain (USDA110 vs. CB1809). This premise is supported by the differential transcriptional changes related to the respiratory pathways in the USDA110-associated nodules and CB1809-associated nodules under LP conditions. Prominent examples of this are the differential expression patterns of genes related to the specialized metabolic pathways, which serve almost exclusively to sustain the cleavage of sugars (i.e., sucrose), phosphorylation of hexoses, glycolysis, Krebs cycle, mETC and carbohydrates storage (starch). These complex transcriptional changes could work in harmony to underpin the acclimatization of soybean to Pi deprivation and optimize nodule metabolism accordingly. However, the potential capacity of nodules to eliminate the adenylate and Pi-dependent biochemical reactions remains decisive under LP conditions. Under these circumstances, USDA110-associated nodules showed alteration in a more significant number of genes (1823) and preferentially employed numerous ATP-dependent respiratory pathways (e.g., HXK, PK, COX and TME) than CB1809-associated nodules under Pi deficiency (645 genes/e.g., MDH, respectively), resulting in lower Pi-stress tolerance and symbiotic efficiency as recently documented by Sulieman et al. (2019). The comparative analysis suggests that soybean possesses considerable respiratory flexibility that might help nodules attenuate the LP availability at the transcriptome level. The induction of various genes related to diverse alternative metabolic pathways was consistent with this proposal. This response includes, for instance, the enhanced coordinated abundance of specific genes involved in the glyoxylate bypass (MLS) and mETC (ETFα/ETFQO system) in CB1809-associated nodules, GABA shunt (calmodulin-binding GAD1) and fermentation (PDC2 and ADH1) in USDA110-associated nodules, and PDH bypass (AAE7/ACN1) in both types of nodules during Pi deficiency. Considering that the present study used the W82-*B. diazoefficiens* USDA110 model platform for dissecting nodule symbiosis, we anticipated that our results could be transformative to upgrade the mechanistic and conceptual understandings of soybean adaptation to Pi deficiency and possibly other N_2-fixing species.

Declaration of generative AI and AI-assisted technologies in the writing process

No AI tools were used during the preparation of this work.

CRediT authorship contribution statement

Saad Sulieman: Conceptualization, Data curation, Formal analysis, Investigation, Methodology, Project administration, Writing – original draft, Writing – review & editing, Supervision, Visualization. **Chien Van Ha:** Data curation, Formal analysis, Methodology. **Dung Tien Le:** Data curation, Formal analysis, Methodology. **Mostafa Abdelrahman:** Data curation, Formal analysis, Methodology. **Cuong Duy Tran:** Data curation, Formal analysis, Methodology. **Yasuko Watanabe:** Formal analysis, Methodology. **Maho Tanaka:** Formal analysis, Methodology. **Zaid Ulhassan:** Data curation, Formal analysis, Methodology. **Mohamed S. Sheteiwy:** Data curation, Formal analysis, Methodology. **Sunil S. Gangurde:** Data curation, Formal analysis, Methodology. **Keiichi Mochida:** Data curation, Formal analysis, Funding acquisition, Methodology. **Motoaki Seki:** Data curation, Formal analysis, Methodology. **Lam-Son Phan Tran:** Conceptualization, Data curation, Formal analysis, Investigation, Methodology, Project administration, Resources, Supervision, Writing – original draft, Writing – review & editing.

Declaration of competing interest

The authors declare that they have no known competing financial interests or personal relationships that could have appeared to influence the work reported in this paper.

Data availability

Data will be made available on request.

Acknowledgments

Saad Sulieman wishes to acknowledge the Japan Society for the Promotion of Science (JSPS) for a postdoc fellowship. We gratefully acknowledge Prof. Peter M. Gresshoff at the University of Queensland (Australia) for providing the *Bradyrhizobium diazoefficiens* USDA110 and CB1809 strains. This work was partially supported by Cabinet Office, Government of Japan, Moonshot R&D Program for Agriculture, Forestry and Fisheries (funding agency: Bio-oriented Technology Research Advancement Institution, No. JPJ009237).

Supplementary materials

Supplementary material associated with this article can be found, in the online version, at doi:10.1016/j.stress.2024.100368.

References

Anthon, G.E., Emerich, D.W., 1990. Developmental regulation of enzymes of sucrose and hexose metabolism in effective and ineffective soybean nodules. Plant Physiol. 92, 346–351.
Approaching Peak Phosphorus, 2022. Nat. Plants 8, 979.
Atkins, C., Smith, P., Mann, A., Thumfort, P., 2001. Localization of carbonic anhydrase in legume nodules. Plant Cell Environ. 24, 317–326.
Baslam, M., Mitsui, T., Sueyoshi, K., Ohyama, T., 2021. Recent advances in carbon and nitrogen metabolism in C3 plants. Int. J. Mol. Sci. 22, 318.
Booth, N.J., Smith, P.M.C., Ramesh, S.A., Day, D.A., 2021. Malate transport and metabolism in nitrogen-fixing legume nodules. Molecules 26, 6876.
Borella, J., do Amarante, L., de Oliveira, D.S.C., de Oliveira, A.C.B., Braga, E.J.B., 2014. Waterlogging-induced changes in fermentative metabolism in roots and nodules of soybean genotypes. Sci. Agric. 71, 499–508.
Chen, L., Qin, L., Zhou, L., Li, X., Chen, Z., Sun, L., Wang, W., Lin, Z., Zhao, J., Yamaji, N., Ma, J.F., Gu, M., Xu, G., Liao, H., 2019. A nodule-localized phosphate transporter GmPT7 plays an important role in enhancing symbiotic N_2 fixation and yield in soybean. New Phytol. 221, 2013–2025.
Coker, G.T., Schubert, K.R., 1981. Carbon dioxide fixation in soybean roots and nodules: I. characterization and comparison with N_2 fixation and composition of xylem exudate during early nodule development. Plant Physiol. 67, 691–696.
Copeland, L., Quinnell, R.G., Day, D.A., 1989. Malic enzyme activity in bacteroids from soybean nodules. J. Gen. Microbiol. 135, 2005–2011.
da-Silva, C.J., do Amarante, L., 2020. Short-term nitrate supply decreases fermentation and oxidative stress caused by waterlogging in soybean plants. Environ. Exp. Bot. 176, 104078.
Day, D.A., Copeland, L., 1991. Carbon metabolism and compartmentation in nitrogen-fixing legume nodules. Plant Physiol. Biochem. 29, 185–201.
Dennis, D.T., Greyson, M.F., 1987. Fructose 6-phosphate metabolism in plants. Physiol. Plant 69, 395–404.
Deroche, M., Carrayol, E., 1988. Nodule phosphoenolpyruvate carboxylase: a review. Physiol. Plant 74, 775–782.

Driscoll, B.T., Finan, T.M., 1996. $NADP^+$-dependent malic enzyme of *Rhizobium meliloti*. J. Bacteriol. 178, 2224–2231.
Fargeix, C., Gindro, K., Widmer, F., 2004. Soybean (*Glycine max* L.) and bacteroid glyoxylate cycle activities during nodular senescence. J. Plant Physiol. 161, 183–190.
Foyer, C.H., Siddique, K.H.M., Tai, A.P.K., Anders, S., Fodor, N., Wong, F.L., Ludidi, N., Chapman, M.A., Ferguson, B.J., Considine, M.J., Zabel, F., Prasad, P.V.V., Varshney, R.K., Nguyen, H.T., Lam, H.M., 2019. Modelling predicts that soybean is poised to dominate crop production across Africa. Plant Cell Environ. 42, 373–385.
García-de los Santos, A., Morales, A., Baldomá, L., Clark, S.R.D., Brom, S., Yost, C.K., Hernández-Lucas, I., Aguilar, J., Hynes, M.F., 2002. The *glcB* locus of *Rhizobium leguminosarum* VF39 encodes an arabinose-inducible malate synthase. Can. J. Microbiol. 48, 922–932.
Georgiev, G.I., Tsvetkova, G.E., 2011. Changes in phosphate fractions, growth rate, nodulation and $nitrogen_2$ fixation of phosphorus-starved soybean plants. J. Plant Nutr. 34, 2055–2068.
Gordon, A.J., Minchin, F.R., James, C.L., Komina, O., 1999. Sucrose synthase in legume nodules is essential for nitrogen fixation. Plant Physiol. 120, 867–877.
Gout, E., Boisson, A., Aubert, S., Douce, R., Bligny, R., 2001. Origin of the cytoplasmic pH changes during anaerobic stress in higher plant cells. Carbon-13 and phosphorous-31 nuclear magnetic resonance studies. Plant Physiol. 125, 912–925.
Green, L., Karr, D., Emerich, D., 1998. Isocitrate dehydrogenase and glyoxylate cycle enzyme activities in *Bradyrhizobium japonicum* under various growth conditions. Arch. Microbiol. 169, 445–451.
Gupta, K.J., Neelwarne, B., Mur, L.A.J., 2015. Integrating classical and alternative respiratory pathways. In: Gupta, K.J., Mur, L.A.J., Neelwarne, B. (Eds.), Alternative Respiratory Pathways in Higher Plants. John Wiley & Sons, Ltd, West Sussex, UK, pp. 3–19.
Juszczuk, I.M., Rychter, A.M., 2002. Pyruvate accumulation during phosphate deficiency stress of bean roots. Plant Physiol. Biochem. 40, 783–788.
Kaneko, T., Nakamura, Y., Sato, S., Minamisawa, K., Uchiumi, T., Sasamoto, S., Watanabe, A., Idesawa, K., Iriguchi, M., Kawashima, K., Kohara, M., Matsumoto, M., Shimpo, S., Tsuruoka, H., Wada, T., Yamada, M., Tabata, S., 2002. Complete genomic sequence of nitrogen-fixing symbiotic bacterium *Bradyrhizobium japonicum* USDA110. DNA Res. 9, 189–197.
Kolbe, A., Tiessen, A., Schluepmann, H., Paul, M., Ulrich, S., Geigenberger, P., 2005. Trehalose 6-phosphate regulates starch synthesis via posttranslational redox activation of ADP-glucose pyrophosphorylase. Proc. Natl. Acad. Sci. U. S. A. 102, 11118–11123.
Kotchoni, S.O., Kuhns, C., Ditzer, A., Kirch, H.H., Bartels, D., 2006. Over-expression of different aldehyde dehydrogenase genes in *Arabidopsis thaliana* confers tolerance to abiotic stress and protects plants against lipid peroxidation and oxidative stress. Plant Cell Environ. 29, 1033–1048.
Lazali, M., Bargaz, A., Brahimi, S., Amenc, L., Abadie, J., Drevon, J.J., 2016. Expression of a phosphate-starvation inducible fructose-1,6-bisphosphatase gene in common bean nodules correlates with phosphorus use efficiency. J. Plant Physiol. 205, 48–56.
Lazali, M., Blavet, D., Pernot, C., Desclaux, D., Drevon, J.J., 2017. Efficiency of phosphorus use for dinitrogen fixation varies between common bean genotypes under phosphorus limitation. Agron. J. 109, 1–8.
Le, D.T., Nishiyama, R., Watanabe, Y., Tanaka, M., Seki, M., Ham le, H., Yamaguchi-Shinozaki, K., Shinozaki, K., Tran, L.S., 2012a. Differential gene expression in soybean leaf tissues at late developmental stages under drought stress revealed by genome-wide transcriptome analysis. PLoS One 7, e49522.
Le, D.T., Aldrich, D.L., Valliyodan, B., Watanabe, Y., Ha, C.V., Nishiyama, R., Guttikonda, S.K., Quach, T.N., Gutierrez-Gonzalez, J.J., Tran, L.S., Nguyen, H.T., 2012b. Evaluation of candidate reference genes for normalization of quantitative RT-PCR in soybean tissues under various abiotic stress conditions. PLoS One 7, e46487.
Le Roux, M.R., Khan, S., Valentine, A.J., 2009. Nitrogen and carbon costs of soybean and lupin root systems during phosphate starvation. Symbiosis 48, 102–109.
Li, H., Xu, L., Li, J., Lyu, X., Li, S., Wang, C., Wang, X., Ma, C., Yan, C., 2022. Multi-omics analysis of the regulatory effects of low-phosphorus stress on phosphorus transport in soybean roots. Front. Plant Sci. 13, 992036.
Liu, A., Contador, C.A., Fan, K., Lam, H.M., 2018. Interaction and regulation of carbon, nitrogen, and phosphorus metabolisms in root nodules of legumes. Front. Plant Sci. 9, 1860.
Liu, S., Zhang, P., Marley, B., Liu, W., 2019. The factors affecting farmers' soybean planting behavior in Heilongjiang Province, China. Agriculture 9, 188.
Lyu, X., Sun, C., Zhang, J., Wang, C., Zhao, S., Ma, C., Li, S., Li, H., Gong, Z., Yan, C., 2022. Integrated proteomics and metabolomics analysis of nitrogen system regulation on soybean plant nodulation and nitrogen fixation. Int. J. Mol. Sci. 23, 2545.
Marillia, E.F., Micallef, B.J., Micallef, M., Weninger, A., Pedersen, K.K., Zou, J., Taylor, D.C., 2003. Biochemical and physiological studies of *Arabidopsis thaliana* transgenic lines with repressed expression of the mitochondrial pyruvate dehydrogenase kinase. J. Exp. Bot. 54, 259–270.
McDermott, T.R., Griffith, S.M., Vance, C.P., Graham, P.H., 1989. Carbon metabolism in *Bradyrhizobium japonicum* bacteroids. FEMS Microbiol. Rev. 63, 327–340.
Mo, X., Liu, G., Zhang, Z., Lu, X., Liang, C., Tian, J., 2022. Mechanisms underlying soybean response to phosphorus deficiency through integration of omics analysis. Int. J. Mol. Sci. 23, 4592.
Møller, I.M., Rasmusson, A.G., Van Aken, O., 2021. Plant mitochondria - past, present and future. Plant J. 108, 912–959.
Nasr Esfahani, M., Kusano, M., Nguyen, K.H., Watanabe, Y., Ha, C.V., Saito, K., Sulieman, S., Herrera-Estrella, L., Tran, L.S., 2016. Adaptation of the symbiotic *Mesorhizobium*–chickpea relationship to phosphate deficiency relies on reprogramming of whole-plant metabolism. Proc. Natl. Acad. Sci. U. S. A. 113, E4610–E4619.
Nendel, C., Reckling, M., Debaeke, P., Schulz, S., Berg-Mohnicke, M., Constantin, J., Fronzek, S., Hoffmann, M., Jakšić, S., Kersebaum, K.C., Klimek-Kopyra, A., Raynal, H., Schoving, C., Stella, T., Battisti, R., 2023. Future area expansion outweighs increasing drought risk for soybean in Europe. Glob. Chang. Biol. 29, 1340–1358.
Oehrle, N.W., Sarma, A.D., Waters, J.K., Emerich, D.W., 2008. Proteomic analysis of soybean nodule cytosol. Phytochemistry 69, 2426–2438.
Ohyama, T., Fujikake, H., Yashima, H., Tanabata, S., Ishikawa, S., Sato, T., Nishiwaki, T., Ohtake, N., Sueyoshi, K., Ishii, S., Fujimaki, S., 2011. Effect of nitrate on nodulation and nitrogen fixation of soybean. In: El-Shemy, H.A. (Ed.), Soybean, Physiology and Biochemistry. InTech Open Access Publisher, Rijeka, pp. 333–364.
Oliver, D.J., Nikolau, B.J., Wurtele, E.S., 2009. Acetyl-CoA—Life at the metabolic nexus. Plant Sci. 176, 597–601.
Prasad, T.K., Stewart, C.R., 1992. cDNA clones encoding *Arabidopsis thaliana* and *Zea mays* mitochondrial chaperonin HSP60 and gene expression during seed germination and heat shock. Plant Mol. Biol. 18, 873–885.
Ribet, J., Drevon, J.J., 1995. Phosphorus deficiency increases the acetylene-induced decline in nitrogenase activity in soybean (*Glycine max* (L.) Merr.). J. Exp. Bot. 46, 1479–1486.
Ricoult, C., Cliquet, J.B., Limami, A.M., 2005. Stimulation of alanine amino transferase (*AlaAT*) gene expression and alanine accumulation in embryo axis of the model legume *Medicago truncatula* contribute to anoxia stress tolerance. Physiol. Plant 123, 30–39.
Rychter, A.M., Szal, B., 2015. Alternative pathways and phosphate and nitrogen nutrition. In: Gupta, K.J., Mur, L.A.J., Neelwarne, B. (Eds.), Alternative Respiratory Pathways in Higher Plants. John Wiley & Sons, Ltd, West Sussex, UK, pp. 53–74.
Schmutz, J., Cannon, S.B., Schlueter, J., Ma, J., Mitros, T., Nelson, W., Hyten, D.L., Song, Q., Thelen, J.J., Cheng, J., Xu, D., Hellsten, U., May, G.D., Yu, Y., Sakurai, T., Umezawa, T., Bhattacharyya, M.K., Sandhu, D., Valliyodan, B., Lindquist, E., Peto, M., Grant, D., Shu, S., Goodstein, D., Barry, K., Futrell-Griggs, M., Abernathy, B., Du, J., Tian, Z., Zhu, L., Gill, N., Joshi, T., Libault, M., Sethuraman, A., Zhang, X.C., Shinozaki, K., Nguyen, H.T., Wing, R.A., Cregan, P., Specht, J., Grimwood, J., Rokhsar, D., Stacey, G., Shoemaker, R.C., Jackson, S.A., 2010. Genome sequence of the palaeopolyploid soybean. Nature 463, 178–183.
Shelp, B.J., Bown, A.W., Zarei, A., 2017. 4-Aminobutyrate (GABA): a metabolite and signal with practical significance. Botany 95, 1015–1098.
Souza, S.C., Mazzafera, P., Sodek, L., 2016. Flooding of the root system in soybean: biochemical and molecular aspects of N metabolism in the nodule during stress and recovery. Amino Acids 48, 1285–1295.
Streeter, J.G., 1991. Transport and metabolism of carbon and nitrogen in legume nodules. Adv. Bot. Res. 18, 129–187.
Subramanian, S., Smith, D.L., 2013. A proteomics approach to study soybean and its symbiont *Bradyrhizobium japonicum* –a review. In: Board, J. (Ed.), A Comprehensive Survey of International Soybean Research. InTech Open Access Publisher, Rijeka, pp. 3–30.
Suganuma, N., Yamamoto, Y., 1987. Carbon metabolism related to nitrogen fixation in soybean root nodules. Soil Sci. Plant Nutr. 33, 79–91.
Sulieman, S., Schulze, J., 2010. Phloem-derived γ-aminobutyric acid (GABA) is involved in upregulating nodule N_2 fixation efficiency in the model legume *Medicago truncatula*. Plant Cell Environ. 33, 2162–2172.
Sulieman, S., Kusano, M., Ha, C.V., Watanabe, Y., Abdalla, M.A., Abdelrahman, M., Kobayashi, M., Saito, K., Mühling, K.H., Tran, L.S., 2019. Divergent metabolic adjustments in nodules are indispensable for efficient N_2 fixation of soybean under phosphate stress. Plant Sci. 289, 110249.
Sulieman, S., Abdelrahman, M., Tran, L.S., 2022. Carbon metabolic adjustment in soybean nodules in response to phosphate limitation: a metabolite perspective. Environ. Exp. Bot. 196, 104810.
Tajima, S., Larue, T.A., 1982. Enzymes for acetaldehyde and ethanol formation in legume nodules. Plant Physiol. 70, 388–392.
Thimm, O., Bläsing, O., Gibon, Y., Nagel, A., Meyer, S., Krüger, P., Selbig, J., Müller, L.A., Rhee, S.Y., Stitt, M., 2004. MAPMAN: a user-driven tool to display genomics data sets onto diagrams of metabolic pathways and other biological processes. Plant J. 37, 914–939.
Tola, A.J., Jaballi, A., Germain, H., Missihoun, T.D., 2021. Recent development on plant aldehyde dehydrogenase enzymes and their functions in plant development and stress signaling. Genes 12, 51.
Toomer, O.T., Oviedo, E.O., Ali, M., Patino, D., Joseph, M., Frinsko, M., Vu, T., Maharjan, P., Fallen, B., Mian, R., 2023. Current agronomic practices, harvest & post-harvest processing of soybeans (*Glycine max*) - a review. Agronomy 13, 427.
Usadel, B., Poree, F., Nagel, A., Lohse, M., Czedik-Eysenberg, A., Stitt, M., 2009. A guide to using MapMan to visualize and compare Omics data in plants: a case study in the crop species, Maize. Plant Cell Environ. 32, 1211–1229.
Valentine, A.J., Kleinert, A., Benedito, V.A., 2017. Adaptive strategies for nitrogen metabolism in phosphate deficient legume nodules. Plant Sci. 256, 46–52.
Vance, C.P., Heichel, G.H., 1991. Carbon in N_2 fixation: limitation or exquisite adaption. Annu. Rev. Plant Physiol. Plant Mol. Biol. 42, 373–392.
Vance, C.P., 2008. Carbon and nitrogen metabolism in legume nodules. In: Dilworth, M. J., James, E.K., Sprent, J.I., Newton, W.E. (Eds.), Nitrogen-fixing Leguminous Symbioses, pp. 293–320.
Vauclare, P., Bligny, R., Gout, E., De Meuron, V., Widmer, F., 2010. Metabolic and structural rearrangement during dark-induced autophagy in soybean (*Glycine max* L.) nodules: an electron microscopy and ^{31}P and ^{13}C nuclear magnetic resonance study. Planta 231, 1495–1504.

Verma, D.P.S., 1989. Plant genes involved in carbon and nitrogen assimilation in root nodules. In: Poulton, J.E., Romeo, J.T., Conn, E.E. (Eds.), Plant Nitrogen Metabolism. Recent Advances in Phytochemistry, 23. Springer, Boston, MA. https://doi.org/10.1007/978-1-4613-0835-5_2.

Vidal, J., Chollet, R., 1997. Regulatory phosphorylation of C_4 PEP carboxylase. Trends. Plant Sci. 2, 230–237.

Wang, L., Liang, J., Zhou, Y., Tian, T., Zhang, B., Duanmu, D., 2021. Molecular characterization of carbonic anhydrase genes in *Lotus japonicus* and their potential roles in symbiotic nitrogen fixation. Int. J. Mol. Sci. 22, 7766.

Weraduwage, S.M., Micallef, M.C., Marillia, E.F., Taylor, D.C., Grodzinski, B., Micallef, B. J., 2016. Increased mtPDH activity through antisense inhibition of mitochondrial pyruvate dehydrogenase kinase enhances inflorescence initiation, and inflorescence growth and harvest index at elevated CO_2 in *Arabidopsis thaliana*. Front. Plant Sci. 7, 95.

Wiederstein, M., Baumgartner, S., Lauter, K., 2023. Soybean (*Glycine max*) allergens – a review on an outstanding plant food with allergenic potential. ACS Food Sci. Technol. 3, 363–378.

Yao, Y., Yuan, H., Wu, G., Ma, C., Gong, Z., 2022. Proteome analysis of the soybean nodule phosphorus response mechanism and characterization of stress-induced ribosome structural and protein expression changes. Front. Plant Sci. 13, 908889.

Zabalza, A., van Dongen, J.T., Froehlich, A., Oliver, S.N., Faix, B., Gupta, K.J., Schmälzlin, E., Igal, M., Orcaray, L., Royuela, M., Geigenberger, P., 2009. Regulation of respiration and fermentation to control the plant internal oxygen concentration. Plant Physiol. 149, 1087–1098.

Zeng, L., Deng, R., Guo, Z., Yang, S., Deng, X., 2016. Genome-wide identification and characterization of glyceraldehyde-3-phosphate dehydrogenase genes family in wheat (*Triticum aestivum*). BMC Genom. 17, 240.

Zhang, G., Ahmad, M.Z., Chen, B., Manan, S., Zhang, Y., Jin, H., Wang, X., Zhao, J., 2020. Lipidomic and transcriptomic profiling of developing nodules reveals the essential roles of active glycolysis and fatty acid and membrane lipid biosynthesis in soybean nodulation. Plant J. 103, 1351–1371.

Zhang, Y., Liang, Y., Zhao, X., Jin, X., Hou, L., Shi, Y., Ahammed, G.J, 2019. Silicon compensates phosphorus deficit-induced growth inhibition by improving photosynthetic capacity, antioxidant potential, and nutrient homeostasis in tomato. Agronomy 9, 733.

Zhang, Y., Chen, H., Liang, Y., Lu, T., Liu, Z., Jin, X., Hou, L., Xu, J., Zhao, H., Shi, Y., Ahammed, G.J, 2021. Comparative transcriptomic and metabolomic analyses reveal the protective effects of silicon against low phosphorus stress in tomato plants. Plant Physiol. Biochem. 166, 78–87.

Zhao, H., Kosma, D.K., Lü, S., 2021. Functional role of long-chain acyl-CoA synthetases in plant development and stress responses. Front. Plant Sci. 12, 640996.

Zhong, Y., Tian, J., Li, X., Liao, H., 2023. Cooperative interactions between nitrogen fixation and phosphorus nutrition in legumes. New Phytol. 237, 734–745.

Zhu, S., Chen, Z., Xie, B., Guo, Q., Chen, M., Liang, C., Bai, Z., Wang, X., Wang, H., Liao, H., Tian, J., 2021. A phosphate starvation responsive *malate dehydrogenase, GmMDH12* mediates malate synthesis and nodule size in soybean (*Glycine max*). Environ. Exp. Bot. 189, 104560.